J. Membrane Biol. 186, 113–129 (2002)
DOI: 10.1007/s00232-001-0140-z

The Journal of
Membrane
Biology

Effects of High Pressure on Glucose Transport in the Human Erythrocyte

R.J. Naftalin[1], I. Afzal[1], J.A. Browning[2], R.J. Wilkins[2], J.C. Ellory[2]
[1]Research Center for Cardiovascular Biology and Medicine, GKT School of Biomedical Sciences, King's College London, Guy's Campus, London SE1 1UL, United Kingdom
[2]University Laboratory of Physiology, Parks Road, Oxford, OX1 3PT, United Kingdom

Received: 6 July 2001/Revised: 9 November 2001

Abstract. The effects of raised hydraulic pressure on D-glucose exit from human red cells at 25°C were determined using light scattering measurements in a sealed pressurized spectrofluorimeter cuvette. The reduction in the rates of glucose exit with raised pressure provides an index of the activation volume, $\Delta V^{\ddagger}$ $(\delta \ln k/\delta P)_{(T)} = -\Delta V^{\ddagger}/RT$. Raised pressure decreased the rate constant of glucose exit from 0.077 ± 0.003 s^{-1} to 0.050 ± 0.002 s^{-1} ($n = 5$, $P < 0.003$). The K_i for glucose binding to the external site was 2.7 ± 0.4 mM (0.1 MPa) and was reduced to 1.45 ± 0.15 mM (40 MPa), ($P < 0.01$, Student's t test). Maltose had a biphasic effect on $\Delta V^{\ddagger}$. At [maltose] <250 μM, $\Delta V^{\ddagger}$ of glucose exit increased above that with [maltose = 0 mM], at >1 mM maltose, $\Delta V^{\ddagger}$ was reduced below that with [maltose = 0 mM]. Pentobarbital (2 mM) decreased the $\Delta V^{\ddagger}$ of net glucose exit into glucose-free solution from 30 ± 5 ml mol^{-1} (control) to 2 ± 0.5 ml mol^{-1} ($P < 0.01$). Raised pressure had a negligible effect on L-sorbose exit. These findings suggest that stable hydrated and liganded forms of GLUT with lower affinity towards glucose permit higher glucose mobilities across the transporter and are modelled equally well with one-alternating or a two-fixed-site kinetic models.

Key words: Glucose transport — Human erythrocytes — Pressure — Hydration — Activation volume

Introduction

Changes in pressure >10–20 MPa can be used to determine the activation volume of chemical processes. The activation volume is defined as the difference in partial molar volume between the activated state and the reactants of a process, $\Delta V^{\ddagger}$ ml mol^{-1}. It is determined from the dependence of the rate-coefficient, k, on pressure, P, using: $(\delta \ln k/\ \delta P)_{(T)} = -\Delta V^{\ddagger}/RT$ (Northrop, 1996). A positive volume change obtains when enzyme-catalyzed rates are diminished on raising pressure and signifies that the chemical process involves a net increase in volume. Pressure-induced volume decreases result from the compressibility of native proteins. Reduction in size of internal cavities constrains small fluctuations in the polypeptide chains, thereby slowing diffusion of mobile molecules through the protein, and hence increases the activation volume of solute diffusion through proteins (Gross, Auerbach & Jaenicke, 1993; Gross & Jaenicke, 1994; Cioni & Strambini, 1999). Higher-pressure of >120 MPa can induce large-scale protein unfolding, which results in increased binding of structured water to the exposed surface. Since this bound water has a higher density than the bulk water, denaturation results in a decreased volume (Svergun et al., 1998). This hydration can increase rates of water penetration within the protein. Thus, raising pressure can have a biphasic effect on rates of solute penetration through proteins. Lower pressures of <100 MPa will tend to reduce the rate of diffusion processes, whereas very high pressures can raise the rates, resulting in positive and negative activation volumes respectively (Gross & Jaenicke, 1994; Cioni & Strambini, 1999).

Solvent interactions can stabilize intermediate transition states in a chemical process. Electrostatic rather than entropic effects are now considered to be the most important interactions stabilizing enzyme transition states (Villa et al., 2000; Northrop & Cho, 2000; Fersht, 1999; Mitchell & Litman, 1999, 2000). In the process of ligand-induced protein unfolding, exposure of charged groups on the protein to solvent

Correspondence to: R.J. Naftalin; email: richard.naftalin@kcl.ac.uk

increases the local dielectric constant and thereby simultaneously diminishes local electrostatic forces, and stabilizes the unfolded state.

A previous study on radiolabelled glucose uptake into human red cells (*zero-trans influx*) at 0°C gave an activation volume of 72 ml mol^{-1}. This was similar to the activation volume found for *accelerated exchange* uptake (Thorne, Hall & Lowe, 1992). However, even at 0°C the rate of glucose transport remains high, so accumulation of radiolabelled glucose inside the cells reduces the precision of these measurements.

Here, we have assessed the effects of pressure on net glucose exit fluxes by adapting the Sen and Widdas (1962) technique of light scattering measurements of glucose exit from human red cells in a thermostatically controlled pressure cell incorporated into a fluorescence spectrometer, as described by Browning et al. (1999).

The experiments described here have been designed to observe the differences between unilateral and bilateral interactions of glucose on the GLUT1 transporter. It was hoped that, in addition to illustrating the effects of glucose interaction on GLUT1 hydration, these experiments could also shed light on the mechanism of net glucose transport—whether the transporter is a single-alternating-site-carrier or a fixed-site transporter.

Low concentrations of the disaccharide D-maltose <250 μM in the external solution accelerate 3-O-methyl-glucoside, (3-OMG) uptake (Sultzman & Carruthers, 1999), whilst higher concentrations of maltose inhibit 3-OMG uptake (Hamill, Cloherty & Carruthers, 1999). Since maltose binds to the transporter with high affinity, but is not transported, these results are consistent with cooperative interactions between the inside and outside sites of the transporter. These effects may be reflected in alterations in the activation volume change for glucose exit by maltose binding to the external site.

Additionally, barbiturates are known inhibitors of glucose transport in red cells (El-Barbary, Fenstermacher & Haspel, 1996; Naftalin & Arain, 1999; Stephenson et al., 2000). Pentobarbital increases the activation energy of glucose transport from ≈40 to ≈75 kJ mol^{-1} and is a less effective inhibitor of glucose exchange than of net transport (El-Barbary et al., 1996). These findings indicate that barbiturates may prevent glucose-dependent conformational changes in the glucose transporter and alter the hydration of the glucose-transporter complex. The activation volume changes with glucose transport in the presence and absence of pentobarbital could elucidate this question.

Finally, sorbose is transported via the glucose transporter although does not share some of the properties of glucose transport, namely accelerated exchange (Naftalin, 1996). For this reason, the effects of L-sorbose and D-glucose on the activation volume of GLUT1 have been compared.

Materials and Methods

Solutions

The composition of phosphate-buffered saline was as follows (mM): NaCl 140; KCl 2.5; $MgCl_2 \cdot 2.0$; Na_2HPO_4/NaH_2PO_4 10. All chemicals including D-glucose, D-maltose, L-sorbose and sodium pentobarbital were obtained from Sigma Chemical (Dorset, UK). All solutions were titrated to pH 7.4 with HCl.

Cells

Fresh human erythrocytes were obtained by venepuncture and washed three times in isotonic saline by repeated centrifugation and resuspension. The cells were then suspended in solutions containing D-glucose at the preloading concentration of 100 mM, final haematocrit 10%. The cells were incubated for at least 2 hr, to allow the sugar to equilibrate with the cell water then re-centrifuged to obtain a thick cell suspension of *ca.* 95% haematocrit. This cell suspension was kept at 4°C until required. Aliquots of prewarmed cell suspension (7.5 μl) were added to a cylindrical fluorescence cuvette containing 3 ml of saline solution, which had been prewarmed to the required temperature. The cuvette was sealed with a flexible plastic stopper that permits rapid pressure equilibration between the pressurized external container and the cell suspension. The cell suspensions were mixed vigorously before placing in the cuvette holder, sealing the pressure container and raising the pressure to the required level. The temperature of the cell suspension was set by a temperature-controlled water circulator and was monitored directly in the cuvette holder.

Photometric monitoring was started within 15 sec of mixing. Insertion of the cell suspension into the pressure cell, closing the seal and raising the pressure to 40 MPa takes between 5–10 sec after mixing. Recording was started at the moment when the pressure was raised to the required level. Data were collected at a rate of 0.33–0.5 points sec^{-1}; each run consisted of 200–2000 data points. The excitation and the emission wavelengths E_{ex} and E_{em} were each 650 nm.

The output was recorded and stored on a computer. The photometric response was found to be approximately linear for osmotic perturbations ±50 mM NaCl. The final glucose concentration in nominally glucose-free solution with this regime is maximally 0.25 mM, which is approximately 10-fold less than the K_m of D-glucose measured here, so contamination of the external solution with glucose has a negligible effect on *zero-trans* D-glucose exit. The hydrostatic pressure in the cuvette was altered with a hydraulic press and monitored using a calibrated scale in the range 1–500 atmospheres. No light-scattering changes were observed on addition of cells that had not been pre-incubated in glucose into glucose-free solutions. Similar light-scattering responses were observed for cells suspended in Tris-buffered (10 mM) solutions at pH 7.4.

The time courses of glucose exit were fitted to mono-exponential curves of the form

$$Y_t = A\exp(-kt) + B,$$

using the curve-fitting program in Kaleidagraph 3.51 (Synergy Software). Y_t is the voltage recorded at time, t (sec); the coefficients A and B are scaling factors and k is the exponential rate coefficient. The rate coefficient k is used to monitor the effects of D-glucose, D-maltose, or pentobarbital on D-glucose exit. The initial rates of D-glucose exit were then calculated from the following equation:

sugar exit rate (mmole $(1\,\text{cells})^{-1}\,\text{sec}^{-1}$) $= Ck$,

where C = loading concentration − external [sugar].

A monoexponential curve gives a very good approximation both to the initial zero-order saturation kinetics when the internal site of the carrier is virtually fully saturated and to the later hyperbolic relationship of flux with cell glucose concentration when intracellular [glucose] decreases to levels closer to the K_m for the internal site. The correlation coefficient r to the best-fit monoexponential curve is usually >0.98. The *zero trans net exit* experiment simply determines the maximal rate of glucose exit from preloaded cells into nominally glucose-free solution when the cells are initially loaded with a fully saturating concentration of glucose. The *infinite cis net exit* is measured by varying the concentrations of glucose in the external solution according to the method of Sen and Widdas (1962). The rates of exit are obtained as above and fitted to the non-linear competitive inhibition equation

$$v = V_{max}K_i/(K_i + S_o),$$

where v is the rate of exit of glucose from the cells, sec^{-1}; V_{max} is the maximal rate with neither glucose nor inhibitor present in the external solution (sec^{-1}); K_i is the concentration of sugar or inhibitor present in the external solution giving half-maximal inhibition of exit rate and S_o is the concentration of sugar or inhibitor (mM) in the external solution. These data are also fitted to this equation using the nonlinear best-fit routine in Kaleidagraph 3.5.

Sorbose Exit

Freshly washed human red cells were loaded with 100 mM L-sorbose at 37°C at least 4 hr prior to use, the time courses of sorbose exit were observed as previously described (Naftalin, 1996; Naftalin & Arain, 1999). Similar fits to those described for glucose exit were obtained at 35°C for L-sorbose exit; however, the time courses of sorbose exit at 35°C are ≈30 × slower than for glucose at 25°C.

Estimation of Activation Volume, $\Delta V^{\ddagger}$

The activation volume $\Delta V^{\ddagger}$ is routinely estimated as follows:

$$\Delta V^{\ddagger} = (RT/\Delta P)\ln\{k_{p(40)}/k_{p(0.1)}\},$$

where $k_{p(0.1)}$ and $k_{p(40)}$ = the exit rates of glucose at 25°C at 1 atmosphere (0.1 MPa) and 400 atmospheres (40 MPa), respectively, ΔP = pressure difference = 30.9 MPa.

Estimation of Reaction Volume, ΔV

The reaction volume ΔV is routinely estimated as follows:

$$\Delta V = (RT/\Delta P)\ln\{K_{p(40)}/K_{p(0.1)}\}$$

(Gross and Jaenicke, 1994),

where $K_{p(0.1)}$ and $K_{p(40)} = 1/K_m$ (M) of glucose at 25°C at 1 atmosphere (0.1 MPa) and 400 atmospheres (40 MPa) respectively ΔP = pressure difference = 30.9 MPa.

Statistics

All the probabilities are estimated from two-tailed Student's t-values for unpaired means. The n values are estimated from the number of degrees of freedom. The means are quoted ± SEM.

Results

Effects of Varying Hydrostatic Pressure on Glucose Exit at 25°C

Sample *zero trans* glucose exits at 0.1 and 40 MPa pressure at 25°C are shown in Fig. 1*a*. The lines are the least-square nonlinear fits using the monoexponential equation described in Methods. The effects of varying pressures between 0.1 and 40 MPa on the rates of glucose exit from human red cells loaded with 100 mM glucose ± pentobarbital (2 mM) are shown in Fig. 1*b*. There was an exponential decrease in rate of glucose exit response in this pressure range. On this basis it was decided to estimate activation volumes from differential effects of pressure between 1 and 400 atmospheres (0.1 and 40 MPa, respectively) as described in Methods.

The current method of monitoring the effects of pressure change on glucose exit rates from human red cells is more sensitive than the equivalent methods for monitoring temperature-dependent changes. At temperatures above 45°C there are concerns about protein denaturation and membrane lipid stability, while at temperatures below 25°C, there are concerns about phase changes in membrane lipid affecting the activation energy of glucose transport (Sen & Widdas, 1962; Carruthers, 1990; Naftalin & Arain, 1999). The effects of pressure changes in the range 0.1–40 MPa are, however, linear at 25°C.

Effects of Varying External [Glucose] at 0.1 MPa and 40 MPa on Glucose Exit Rates Infinite *Cis* K_i of Glucose Binding and Activation Volumes, $\Delta V^{\ddagger}$

The effects of varying external [glucose] on the rates of glucose exit at 0.1 MPa and 40 MPa pressure are shown in Fig. 2. Raised pressure reduced the maximal rate of glucose exit from 0.077 ± 0.003 sec^{-1} to 0.050 ± 0.002 ($n = 5$, $P < 0.003$). The K_i for glucose binding to the external site obtained in this study was 2.7 ± 0.39 mM at 0.1 MPa. This value was significantly reduced to 1.45 ± 0.15 mM at 40 MPa ($P < 0.01$, Student's t-test).

Reductions in both V_{max} and K_i by raised pressure are consistent with a pressure-dependent mixed inhibition of transport. With 100 mM glucose in the initial loading condition inside the cell, raising the external glucose from 0 to 10 mM increased the activation volume of glucose exit from 27 ± 1 ml mol^{-1}, with zero mM external [glucose], to 62 ± 10 ml mol^{-1} with 10 mM glucose in the external solution ($P < 0.01$). The doubling of the activation volume of net glucose flux with raised external [glucose] >5 mM indicates that there was additive glucose binding at internal and external sites. The reaction volume ΔV of glucose binding to the external site = −38.6 ± 6.9 ml mol^{-1}.

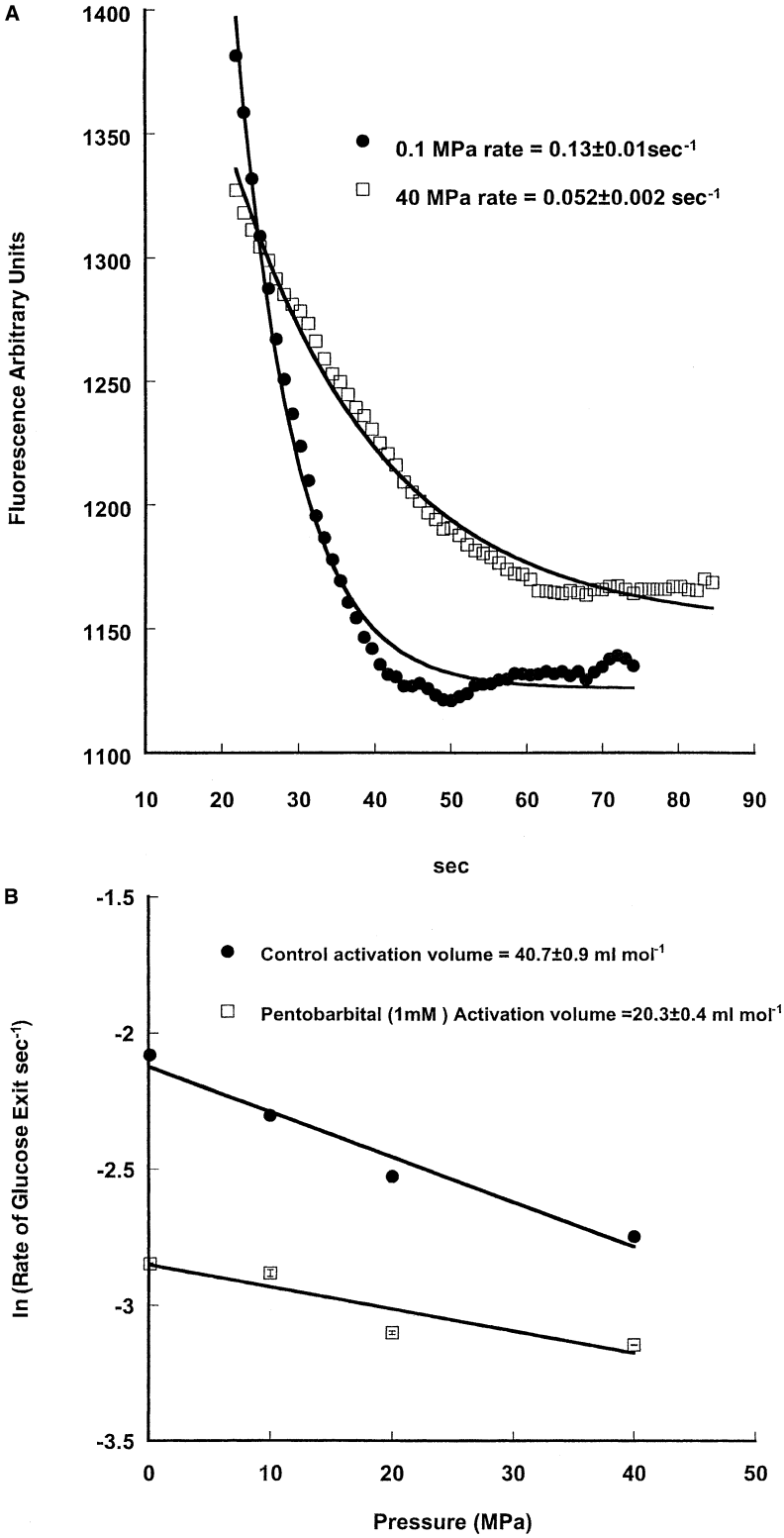

Fig. 1. (*A*) Pressure (40 MPa) reduces the maximal rate of glucose exit from human red cells into glucose-free solution at 25°C. Typical light scattering traces cells preloaded with 100 mM glucose and added to isotonic PBS with zeroglucose at $t = 0$ sec, 25°C, ± high pressure. The rates of glucose exit are estimated here by fitting observed rates of glucose exit to the monoexponential equation $Y = A\exp(-kt) + B$, where A and B are scaling factors and k is the rate coefficient of glucose exit. These constants are obtained by using the nonlinear fitting procedures in Kaleidagraph (Synergy Software). (Open squares) Glucose exit at 40 MPa rate constant 0.13 ± 0.1 sec^{-1}. (*Filled circles*) Glucose exit at 1 atmosphere (0.1 MPa). (*B*) The effects of variable hydrostatic pressure on glucose exit at 25°C ± pentobarbital (1 mM) at 25°C. A plot of the rate constant of glucose exit from human red cells ln (k) versus pressure (MPa) gives an exponential decrease in rate both in controls (*filled circles*) and in cells treated with pentobarbital 1 mM (*open squares*). Error bars shown are SEM. Each point is the mean of 3–5 measurements, made using at least 2 different blood samples. The slope of the linear regression line is an estimate of the change in activation volume, $\Delta V^{\ddagger}$ ml mol^{-1}.

Effects of Maltose in the External Bathing Solution on Pressure-Dependent Glucose Exit

Raising external [maltose] from 0 to 2.5 mM reduced glucose exit rates; the rate constant k of glucose efflux fell from 0.077 sec^{-1} to 0.049 ± 0.004 sec^{-1} ($P < 0.01$); the K_i of maltose-dependent inhibition of glucose exit fell from 0.23 ± 0.06 mM at 0.1 MPa to 0.05 ± 0.02 mM at 40 MPa, ($P < 0.005$) (Fig. 3). At both 0.1 MPa and 40 MPa the inhibition of glucose

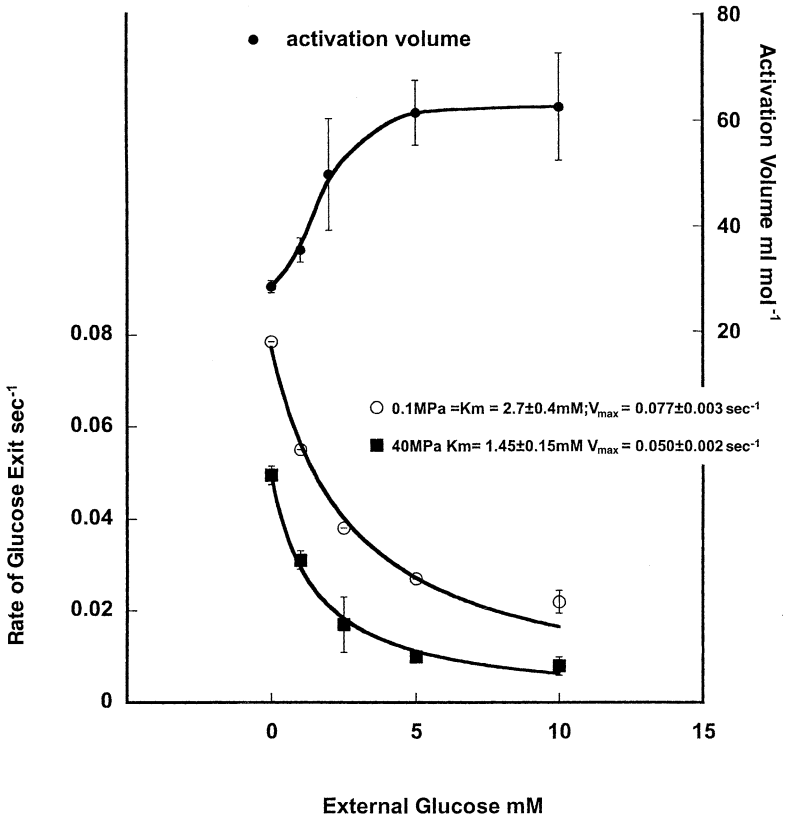

Fig. 2. The effects of hydrostatic pressure change on the kinetic parameters of glucose exit at 25°C. The effects shown are of varying [glucose] and pressure (0.1 MPa, *open circles*; 40 MPa, *filled squares*) in the external solution on the rates of glucose exit from cells loaded initially with 100 mM glucose. Pressure of 40 MPa reduces K_i from 2.7 ± 0.39 mM at 0.1 MPa to 1.45 ± 0.15 mM at 40 MPa ($P < 0.01$, Student's t test). Raised pressure reduces the maximal rate of glucose exit from 0.077 ± 0.003 sec^{-1} to 0.050 ± 0.002 ($n = 5$, $P < 0.003$). The lines are obtained by nonlinear best fit to the observed data points, which are the average of 3–4 experiments, with each experiment consisting of at least 2 observations. The activation volumes of glucose flux (*filled circles*) are plotted as a function of external glucose.

exit was incomplete. Above 3 mM maltose, no further decrease in glucose exit rates was observed. The overall effect of maltose addition to the external solution was to reduce the activation volume of glucose exit from 27 ± 1 ml mol^{-1} with zero [maltose] to 16 ± 5 ml mol^{-1} at 1–2.5 mM maltose ($P < 0.01$). There was a small increase in activation volume at low external [maltose] ($P < 0.05$). The maximal increase was observed with 0.1 mM maltose in the external solution. Raised pressure caused a sharp increase in the apparent affinity of maltose for the external site. The K_i at 0.1 MPa = 0.23 ± 0.06 mM, whereas it dropped to 0.049 ± 0.02 mM when the pressure was raised to 40 MPa ($P = 0.02$, Fig. 3). The reaction volume of maltose binding to the external site = −96 ± 9 ml mol^{-1}.

The biphasic changes in activation volume with increasing external maltose suggest that maltose binds to two classes of external sites. Low maltose concentrations <250 μM increased the activation volume of glucose transport from 25 ml mol^{-1} to 34 ml mol^{-1} ($P < 0.02$). This is similar to the effects of external glucose increasing the activation volume of glucose exit (*see* Fig. 2).

With maltose >1.0 mM the activation volume was significantly less than that when no maltose was present ($P < 0.02$). These effects are consistent with the view that maltose binding to the external site has an allosteric effect on the ligand interaction with the internal sites of the transporter (Sulzman & Carruthers, 1999; Hamill et al., 1999).

Effects of Pentobarbital on Glucose Exit

At atmospheric pressure pentobarbital has a mixed inhibitory effect on net glucose exit from red cells (Naftalin, 1996; Naftalin & Arain, 1999). Pentobarbital inhibited glucose exit, K_i = 0.95 ± 0.08 mM (0.1 MPa) (Fig. 4). Raised pressure (40 MPa) increased the K_i of pentobarbital to 2.57 ± 0.24 mM ($P < 0.01$) whilst it reduced the maximal rate of glucose exit as shown in Figs. 2 and 3. Pentobarbital (2 mM) decreased the activation volume of net glucose exit into glucose-free solution from 30 ± 5 ml mol^{-1} (control) to 2 ± 0.5 ml mol^{-1} ($P < 0.01$). The complete absence of any activation volume change with glucose transport in the presence of pentobarbital (2 mM) (Fig. 4), indicates that the hydration of the transporter of 30 ml mol^{-1} induced by intracellular glucose is dependent on a conformational change that can be inhibited by pentobarbital and to some extent maltose. This demonstrates that the "hydration response" to changes in glucose concentration is not a stoichiometric function of glucose binding, but is dependent on a conformational change that can be modified by external variables. The reaction volume of pentobarbital binding = 60.1 ± 7.7 ml mol^{-1}.

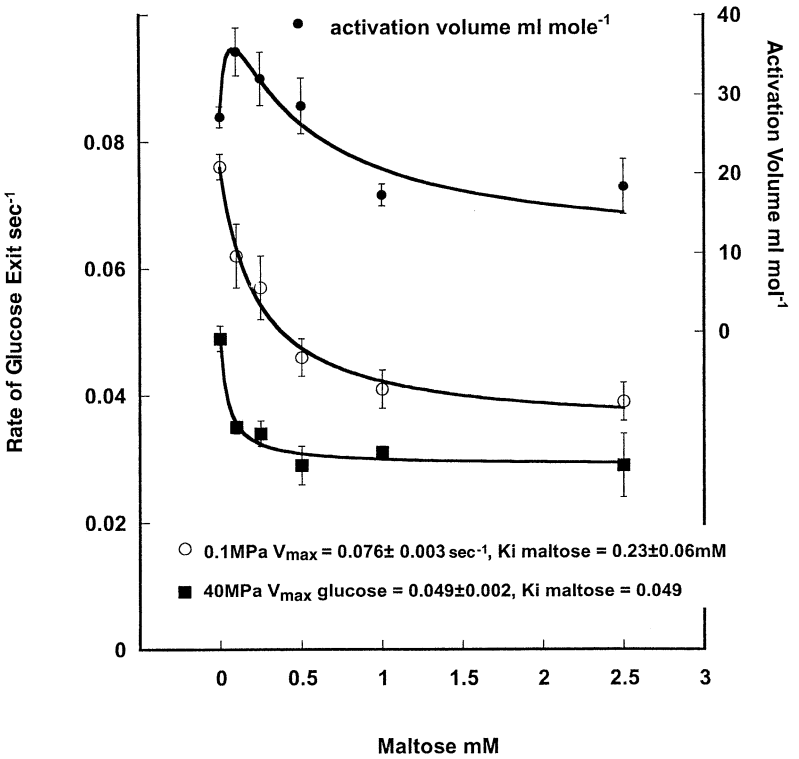

Fig. 3. Effect of D-maltose in the external solution on glucose exit and the activation volume of glucose transport. The effects of varying external maltose from 0–2.5 mM on glucose exit rates ± SEM at 0.1 MPa, (*open, circles*) and at 40 MPa, (*filled squares*). The K_i of maltose-dependent inhibition = 0.23 ± 0.06 mM at 0.1 MPa. At 40 MPa, the K_i of maltose-dependent inhibition of glucose exit falls to 0.049 ± 0.02 mM V_{max} of glucose exit falls from 0.077 sec^{-1} at 0.1 MPa to 0.049 ± 0.004 sec^{-1} at 40 MPa ($P < 0.01$). The $\Delta V^{\ddagger}$ of glucose exits decreases 27 ± 1 ml mol^{-1} with zero maltose to 16 ± 5 ml mol^{-1} at 1–2.5 mM maltose. The data also show an increase in activation volume at external [maltose] < 0.2 mM ($P < 0.05$).

Effects of Pressure on L-Sorbose Flux

The effect of raising pressure from 0.1 MPa to 40 MPa on sorbose exit from red cells at 35°C is negligible. Exit rate at 0.1 MPa = 0.0025 ± 0.0004 ($n = 5$); at 40 MPa, exit rate = 0.0028 ± 0.0004 ($n = 5$). Hence, there is no significant change in activation volume occurring during L-sorbose exit. The $\Delta V^{\ddagger} = 0$ during *zero-trans* L-sorbose transport demonstrates that the $\Delta V^{\ddagger}$ seen during *zero trans* net glucose is a response to a glucose-specific conformational change in GLUT1.

Discussion

Interpretation of the Results

The results indicate that during *zero trans net exit*, with glucose saturating the internal site of the GLUT1 transporter, the activation volume change of the glucose transporter at 25°C is 28–35 ml mol^{-1}, (Figs. 2, 3 and 4). This increase in activation volume is reduced to 2.0 ± 0.5 ml mol^{-1} by pentobarbital (2 mM) (Fig. 4) and to 15 ml mol^{-1} by externally bound maltose (> 1 mM) (Fig. 3). When 100 mM L-sorbose is substituted for D-glucose, there is no activation-volume change. The absence of change in activation volume during L-sorbose transport indicates that the activation-volume change is a specific change caused by glucose-dependent changes in GLUT1 conformation.

These results show that the activation-volume changes are not stoichiometrically coupled responses to glucose binding and transport, but can be modulated by stereospecific interactions within the transporter. Raising external [glucose] from 0–10 mM, as well as reducing the rate of net glucose exit, also raises the activation volume from ≈30 ml mol^{-1} to ≈60 ml mol^{-1} ($P < 0.001$).

The doubling of the activation volume increase when both sides of the transporter are nearly saturated with glucose, (*infinite cis exit*), indicates that D-glucose binds to similar kinds of sites on both sides of the GLUT1 transporter. These findings are equally consistent with separate sites for binding of glucose and water on both sides of the membrane, or a single alternating site, the distribution of which changes with the distribution of ligand on either side of the membrane.

Glucose-Water Interactions with the GLUT1

A number of papers have suggested that water interacts with GLUT1. This interaction may, or may not alter water permeability; (Zeidel et al., 1992; Mannuzzu, Moronne & Macey, 1993; Fischbarg et al., 1994). There is structural evidence that water binds to GLUT1 (Zeng et al., 1996), evidence from solvent-replacement studies of H_2O with D_2O that water reduces glucose transport rates (Naftalin & Rist, 1991), and evidence that replacement of H_2O with alcohols also reduces glucose transport (Widdas

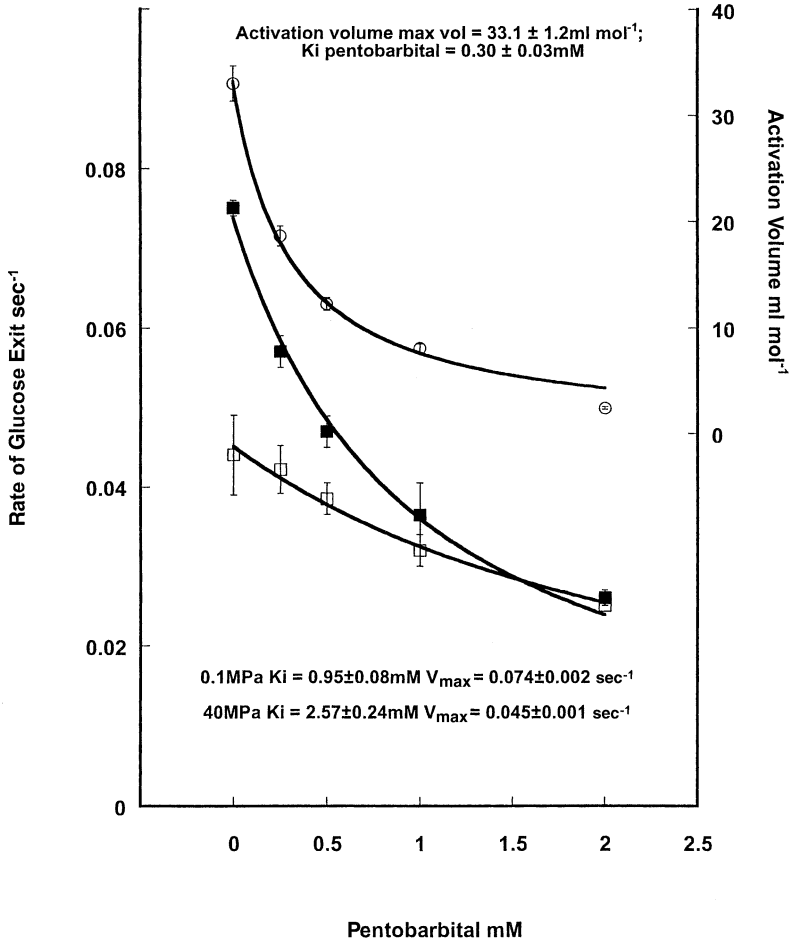

Fig. 4. Effects of pentobarbital on D-glucose exit. Pentobarbital inhibits glucose exit, K_i = 0.95 ± 0.08 mM at 0.1 MPa (*filled squares*). Raised pressure (40 MPa) increases the K_i of pentobarbital to 2.57 ± 0.24 mM ($P < 0.01$). The maximal rate of glucose exit is reduced by raised pressure from 0.074 ± 0.002 sec^{-1} to 0.045 ± 0.01 sec^{-1}. The activation volume of net glucose exit into glucose-free solution (*filled circles*) decreases from 30 ± 5 ml mol^{-1} with 2 mM pentobarbital present ($P < 0.01$).

& Baker, 1998; Baker & Widdas, 1991). NMR studies at low temperatures have shown that the unfrozen water in red cell membranes increases in the presence of glucose and was inhibited by cytochalasin B, indicating that specific glucose binding to GLUT in red cell membranes increases the amount of tightly bound water (Naftalin & Holman, 1977). The latter findings still require to be correlated with the various modes of glucose transport. The activation energy of conformational change in isolated hydrated GLUT1 is lower when liganded to glucose than in the unhydrated form (Appleman & Lienhard, 1989). Additionally, Thorne et al. (1992) demonstrated an activation volume increase of 70–75 ml mol^{-1} during both exchange and net uptakes of labelled glucose into human red cells at 0°C. However, they were unable to show any difference in activation volume between net and exchange uptake, perhaps because the inside sites were fully saturated during the period of observation of net uptake.

The Problem of Pressure-dependent Mixed Inhibition of Glucose Exit

The reduction of the K_i (K_m) of glucose interaction at the external surface from 2.7 ± 0.4 mM to 1.45 ± 0.15 mM on raising pressure from 0.1 to 40 MPa reaction volume $\Delta V = -38.6 \pm 6.9$ ml mol^{-1} ($P < 0.01$) leads to a pressure-dependent enhancement of glucose entry at low $[glucose]_{ext}$. This is apparently a consequence of a pressure-dependent increase in glucose affinity for the external site, leading to enhanced glucose entry. However, this does not explain why high pressure also reduces the maximal rate of *zero trans* net glucose exit when external [glucose] is zero (Figs. 2–4).

A simple Michaelis-Menten formulation of the parameters of net glucose transport is

$$G + C \underset{k_1}{\overset{k_{-1}}{\leftrightarrow}} GC \overset{k_2}{\rightarrow} G + C$$

where k_1 and k_{-1} are the rates of association and dissociation, respectively, of the glucose ligand, G, in solution with its adjacent transporter site C, and k_2 is the unidirectional rate of transport of G across the transporter; $K_m = (k_{-1} + k_2)/(k_1)$; the ratio k_{-1}/k_1 is the dissociation constant, K_d (mM) of glucose for the transporter site. At saturating concentrations of G, k_2 approximates to V_{max} of transport when the *trans site* is vacant. Only when rates k_{-1}, k_1 and k_2 are of the same order of magnitude, will inhibition of k_2 alone affect K_m significantly. If the rates k_{-1}, k_1 are three

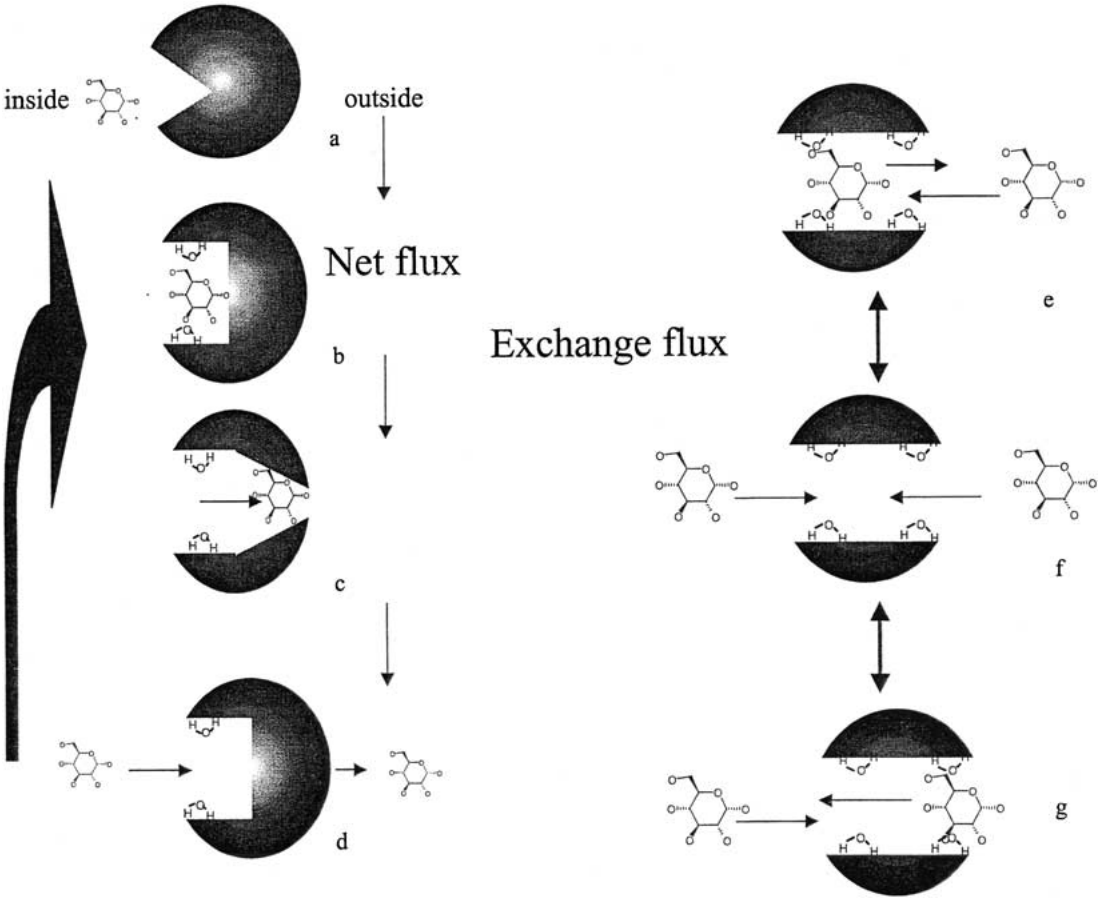

Fig. 5. Model of net and exchange modes of glucose transport via a hydrated GLUT1 "pore". Glucose-dependent effects on GLUT1 hydration and activation of mobility across the transporter. (*a*) Glucose binds to high-affinity inside site of GLUT1; (*b*) the binding induces a conformational change that permits hydration of the site; (*c*) the affinity of glucose is reduced and mobility is increased, permitting transient opening of the *trans* site; (*d*) net transport is completed but the *cis* sites remain hydrated so that glucose transport is facilitated. This leads to an increase in activation volume at the inside sites. The presence of glucose in solutions bathing both sides, (e), results in hydration of both inside and outside sites of GLUT1 with increased mobility (*f*) during net and exchange fluxes, and in an increase in activation volume.

orders of magnitude faster than k_2, as with nucleotide binding to the mitochondrial ATP/ADP carrier (Huber, Klingenberg & Beyer, 1999), or glucose binding to isolated GLUT1 (Janoshazi & Solomon, 1993), then 50% reduction of k_2 (V_{max}) should have negligible effect on K_m or K_d. Similarly, when k_{-1} and $k_1 \gg k_2$, increasing K_d and K_m by 50% by increased rates of dissociation, k_{-1} relative to k_1, will not affect V_{max} significantly.

A New Model for Glucose Transport, in which Hydration Stabilizes the Low-Affinity Activated State of Glucose Binding to the Transporter

Reciprocal Effects of Pressure on Solvent and Solute Binding to GLUT1

A single explanation is required for the combined pressure-dependent decreases in V_{max} of *zero trans net* glucose exit and K_i of *infinite cis* glucose exit at the external surface and the associated increased $\Delta V^{\ddagger}$ with raised external [glucose] (Fig. 2). One possibility is that the glucose-dependent $\Delta V^{\ddagger}$ of GLUT1 results in stable hydrated substates that have higher mobility between the two sides of the transporter than the unhydrated forms (Figs. 5–19).

Glucose binding to GLUT1 at either inside or outside sites will cause localized protein unfolding with resulting hydration of the exposed amino-acid residues in the vicinity of the bound ligand. The enhanced accessibility of water with consequent shielding of the electrostatic forces (Villa et al., 2000; Northrop & Cho, 2000; Fersht, 1999; Mitchell & Litman, 2000) will reduce glucose affinity and increase its mobility within the transporter. Bilateral glucose binding would increase glucose mobility at least twice as much as unilateral binding. Unfolding will increase water binding to the exposed charged residues. This enhanced solvent-binding energy will compensate for the loss of glucose-binding energy

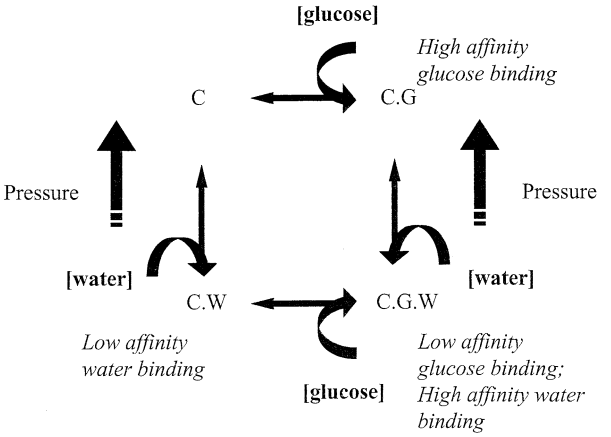

Fig. 6. Model of unilateral glucose and water interactions with GLUT1. Glucose binds to the empty site *C* to form high-affinity glucose-bound site *C.G*. This results in a conformational change (unfolding), which permits water binding to site *C.G.W* and this lowers the affinity of glucose binding to the site and also increases its mobility. However, because of the relatively high affinity of water-binding the site is stable. On glucose dissociation water remains bound but with lower affinity, hence the state *C.W* is relatively unstable and water readily dissociates from it to complete the thermodynamic cycle. Raised hydrostatic pressure reduces the affinity of water for the unfolded state by retarding protein unfolding and thereby promotes the high affinity and low mobility glucose binding state *C.G*.

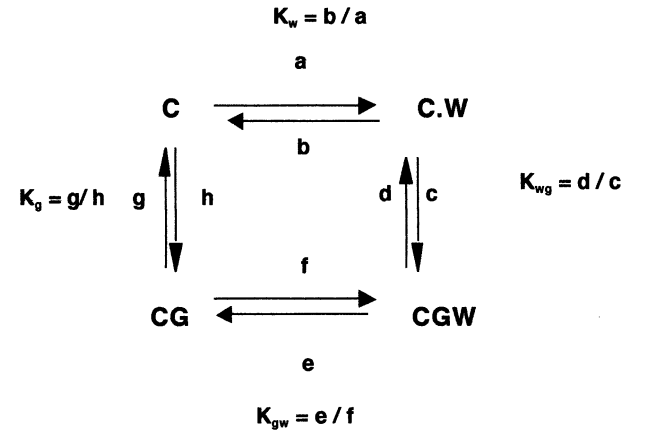

Fig. 7. Glucose and water interactions at a single site using the conventional carrier scheme.

due to shielding of the electrostatic charges and thereby stabilize the transition or "activated state".

Timasheff (1998) has described a model for water-solute interactions with macromolecules. The measured overall binding constant of ligand and water binding $K_b = K_1/K_w$, where K_1 is the binding constant of ligand in the absence of water and K_w is the binding constant of water in the absence of ligand.

Osmotic pressure has recently been used to measure the change in protein hydration with ligand interaction (Parsegian, Rand & Rau, 2000; Rand et al., 1993). Raising osmotic pressure using polyethylene glycol (mw >1000) by 2×10^7 dynes cm^{-2} (2 MPa) results in dehydration of the glucose-binding site and an increase in the affinity of glucose for hexokinase of approximately 5.5-fold (Reid & Rand, 1997).

Thus, there are obvious similarities between the effects of raised hydrostatic pressure on the affinity of glucose and maltose for the glucose transporter observed here and the effects of osmotic pressure on affinity of glucose for hexokinase.

Glucose-water interactions on the GLUT1 transporter can be modelled as a thermodynamic cycle (Timasheff, 1998; White & Wimley, 1999; Parsegian et al., 2000). The steps involve a glucose-dependent conformational change leading to unfolding and solvation of the exposed groups as follows (Figs. 6–10):

Step 1: glucose binds to the folded site.
Step 2: protein unfolds and hydrates with loss of affinity of "voids" within the protein and gain of flexibility of the transporter and gain of mobility of glucose within the transporter (Cioni and Strambini 1999).
Step 3: glucose dissociates from unfolded hydrated GLUT1.
Step 4: refolding and dehydration of GLUT1.

Microscopic reversibility requires that the products of rate coefficients, $aceg = hfdb$ and the energy loss due to decreased glucose-binding affinity on transition from basal and hydrated states are exactly compensated by energy gained from hydration of the exposed site.

Hence, $bd/ac = eg/hf$; and thus $K_wK_{wg} = K_gK_{gw}$. Only three of the four dissociation constants are independently determined.

Thus, $K_{gw} = K_wK_{wg}/K_g$, where K_w, K_g are the dissociation constants of water and glucose for the transporter *C*, and K_{wg} and K_{gw} are dissociation constants of glucose from the water-bound site and of water from the glucose-liganded site, respectively.

Raising pressure from 0.1 MPa to 40 MPa reduces glucose-dependent increases in GLUT1 activation volume and decreases the reaction volume of glucose binding to the external surface of GLUT1. If compression reduces the rate of penetration of water and glucose into surface crevasses in the transporter and increases the resistance to volume increase, it should slow the mobility of glucose across the transporter and reduce glucose-induced hydration within the depths of the transporter. The K_m of glucose interaction with the transporter should thereby be decreased.

An analogue of this process is the pressure-dependent decrease in the rate of quenching of tryptophan phosphorescence in alcohol dehydrogenase and alkaline phosphatase by acrylamide (Cloni & Strombini, 1999). This is thought to result mainly

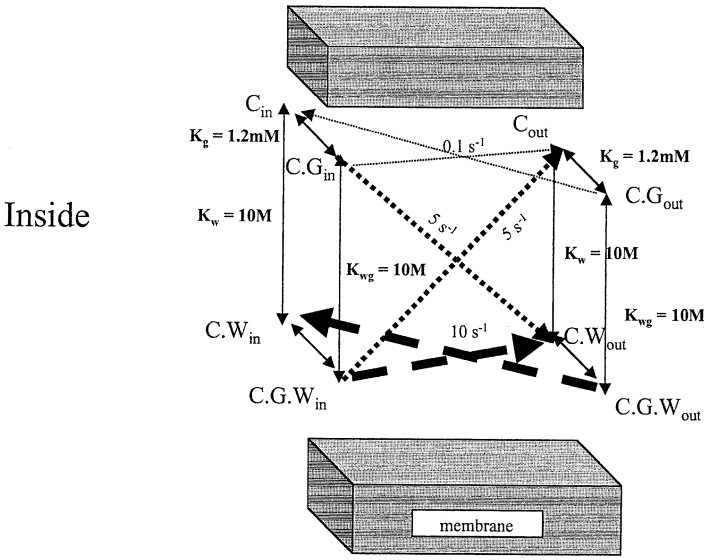

Fig. 8. Diagram of glucose transport across the two-site GLUT1 transporter with bilateral activated sites containing bound water. Modes of glucose transport between bilateral-hydration-stabilized sites in GLUT1. The two-hydrated site model of glucose interaction indicates that there are three common modes of glucose translocation from inside to outside sites or vice versa. The slowest mode (*i*) is when glucose bound to the high-affinity site, $C.G_{in}$ moves to an unhydrated external site to become $C.G_{out}$. The intermediate mode (*ii*) is found in *zero trans* net exit when glucose moves from a hydrated site $C.G.W_{in}$ to a vacant unhydrated site C_{0out} to form $C.G_{out}$, or from an unhydrated site $C.G_{in}$ to a vacant hydrated site $C.W_{out}$ to form $C.G.W_{out}$. The fastest mode (*iii*) obtains during accelerated exchange or *infinite cis* net exits when glucose moves from a hydrated site $C.G.W_{in}$ to a hydrated site $C.W_{out}$.

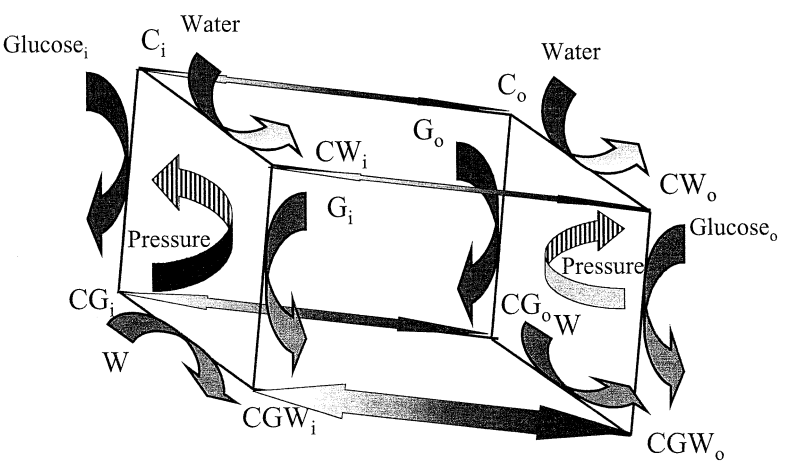

Fig. 9. Carrier model of glucose transport between two sides where the site may be hydrated and or liganded to glucose. The model shown illustrates the substates of the carrier on both sides, the affinities of glucose and water, which are symmetrical, and the rates of translocation of the various forms across the carrier. The rates are those giving a best fit to the data in Fig. 2*A* and are those used for the simulations in Fig. 10.

from pressure-dependent occlusion of free volume within the proteins.

At first sight, ligand-dependent unfolding of protein might seem to be an inappropriate model for the glucose-dependent effects observed here. High pressure >120 MPa is known to cause denaturation of proteins (Gross & Jaenicke, 1994). Protein denaturation exposes more surface to water. This bound water has a higher density than bulk water (Svergun et al., 1998). Consequently, pressure would seem associated with a decreased activation volume rather than an increase, as required of glucose-GLUT1 interactions.

However, some hydrophilic solutes like trehalose, glycerol and glucose stabilize proteins against denaturation, cryoprotect cells and increase the amount of immobilized water within cells (Xie & Timasheff, 1997). Water in contact with hydrophilic surfaces, like SiO_2, has a significantly lower density than bulk solution as a result of depletion of intra-aqueous H-bonds due to preferential bonding of water to the SiO_2 (Hartnig et al., 2000). Thus, partial unfolding induced by hydrophilic ligands can increase the activation volume as a result of the preferential binding of water to the hydrophilic cosolvent (Ebel, Eisenberg & Ghirlando, 2000; Xie & Timasheff, 1997; Timasheff, 1998).

The hydrated forms of both the alternating-mobile-site carrier or the two-fixed-site transporters

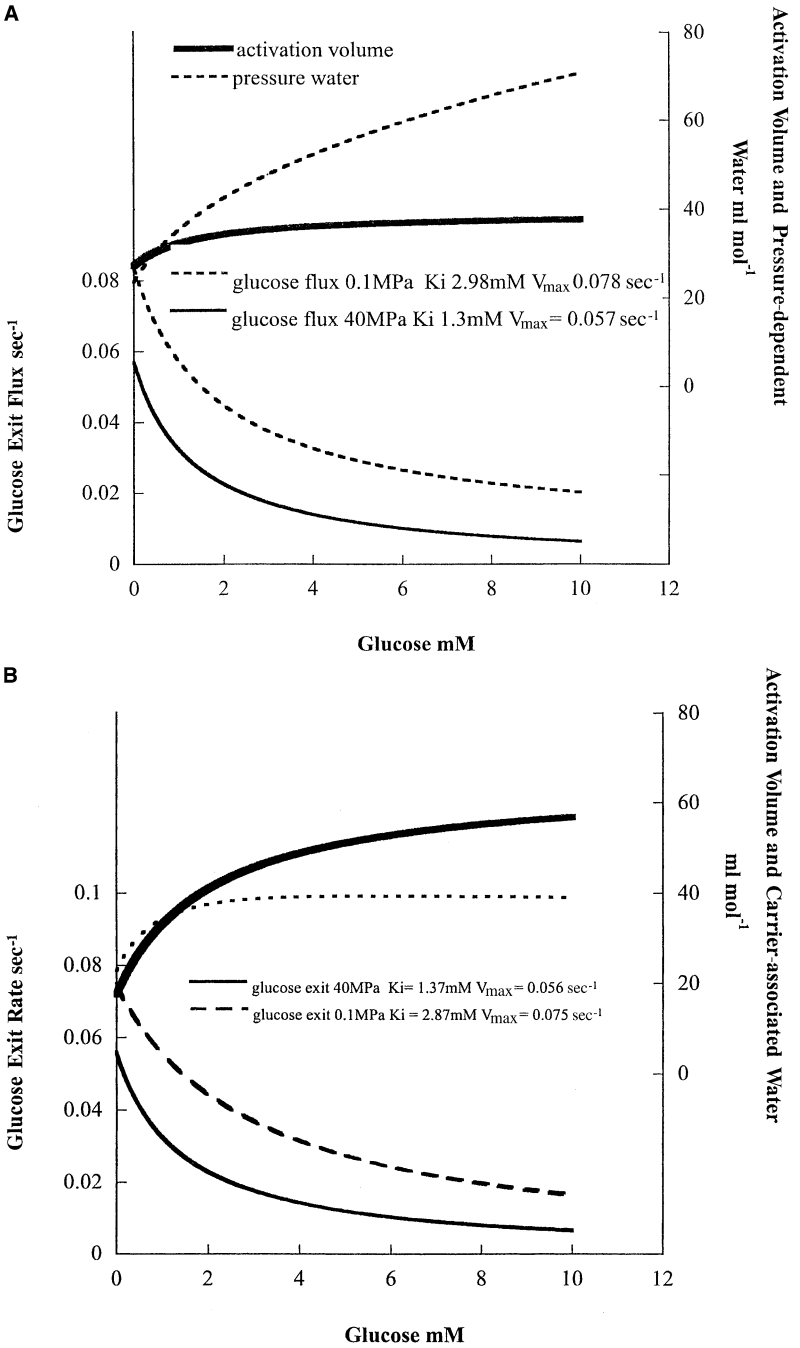

Fig. 10. Simulation of effects of pressure on glucose exit kinetics and activation volume. (*A*) Simulation with two-fixed-sites model of pressure effects on glucose exit from human red cells at 25°C. (*B*) Simulation of effects of pressure change on glucose exit and on activation volume with carrier model. Glucose exit flux was simulated using Berkeley Madonna version 8.01 (URL http:///www.Berkeleymadonna.com), using the kinetics generated by the model described in Figs. 8 and 9. Table 2 gives the parameters used. The relative rates of dehydrated intersite transfer, monhydrated site transfer and bihydrated sites are k_1, k_2 and k_3, respectively, (*see* Fig. 8). The simulated K_i for [glucose] inhibition at the external site at 0.1 MPa = 2.74 mM, V_{max} = 0.072 sec^{-1} (thin continuous line), and at 40 MPa, K_i = 0.98 mM, V_m = 0.054 sec^{-1} (thin broken line) estimated using Kaleidagraph (Synergy Software). The simulated activation volumes as estimated by formula (*see* Methods) increase from 21 ml mol^{-1} at 0 mM external glucose to 70 ml mol^{-1} at 10 mM external glucose. The pressure-displaceable water obtained from the total hydration sites on the model at full saturation on each side equals 36 ml mol^{-1}. These results are essentially identical to those observed in Fig. 2 and indicate that the model is consistent with the data. The parameters for carrier transport are: R_w = rate of hydrated carrier flux; R_g, rate of unhydrated glucose-liganded carrier flux; R_{gw} rate of hydrated glucose carrier flux. The affinities have the same meaning for both models.

simulate equally well the effect of raised pressure from 0.1 MPa to 40 MPa by a reduction in water affinity for the transporter *CW* and glucose-water-transporter complex, *CGW* (*see below*). This effect is an analogue of the effects of pressure-dependent loss of flexibility of protein, which retards activation-volume increases. Raising pressure from 0.1 MPa to 40 MPa is simulated in both models by a reduction in water affinity for the transporter *CW* and glucose-water-transporter complex, *CGW*. A change in notional values of K_w and K_{gw} from 5–10 M H_2O at 0.1 MPa to 20–25 M H_2O at 40 MPa when the glucose concentration = 10 mM, K_g = 1 mM, and water concentration ≈55.5 M (Figs. 10, 11, and 12), reduces the K_{wg} from ≈3 mM to 0.5 mM.

If glucose mobility across the transporter is increased by hydration, raised pressure will also reduce the V_{max} of *zero trans* net glucose exit.

Modeling the Effects of Hydrostatic Pressure on Glucose Fluxes: an Alternating Carrier Model or a Fixed Two-Site Model

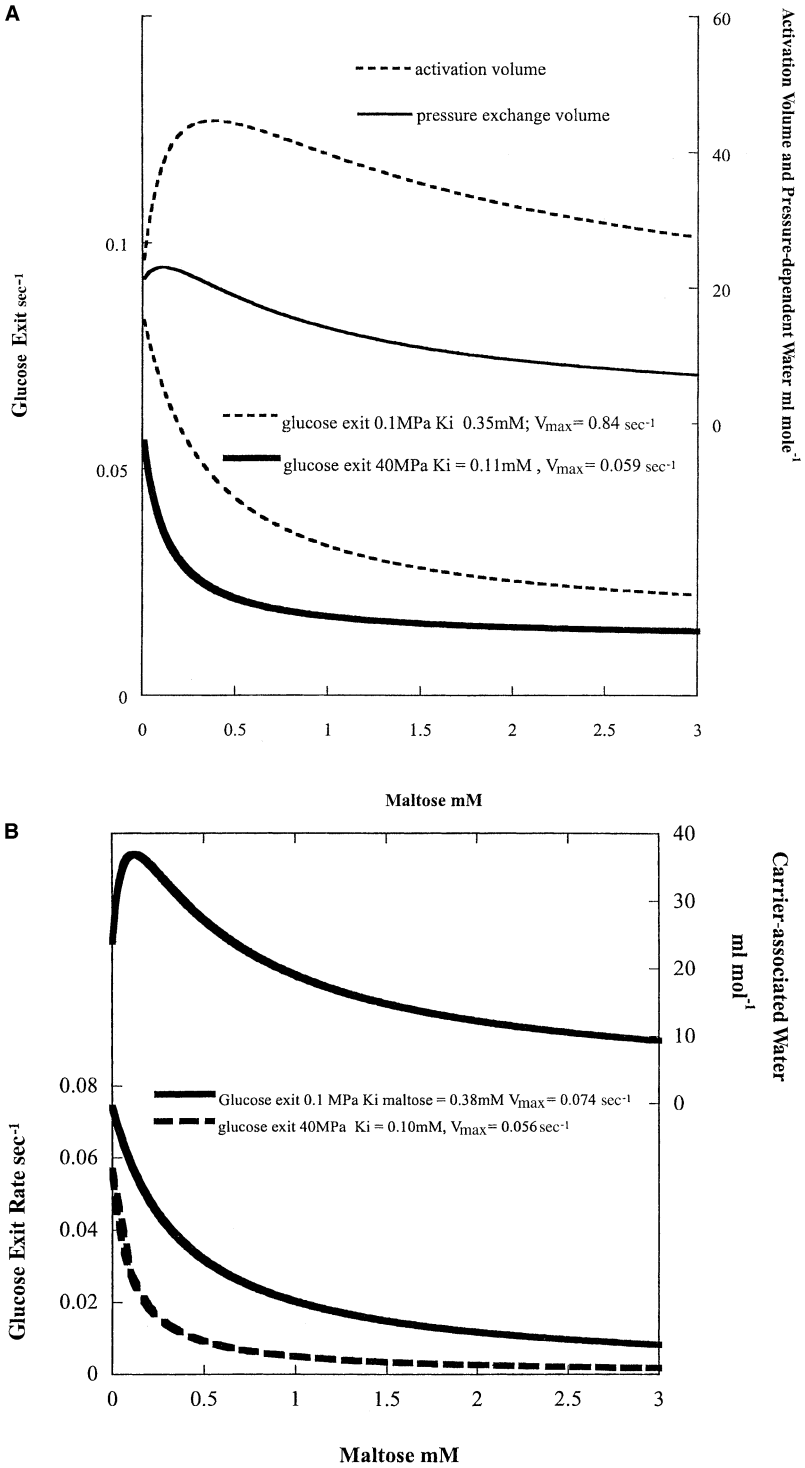

Fig. 11. Simulation of effects of pressure and external maltose on glucose exit kinetics and activation volume. (*A*) Simulation of two-site model of pressure effects on maltose inhibition of glucose exit at 25°C. (*B*) Simulation of effect of maltose on glucose exit and amount of water associated with the 10-state carrier. Inhibition of glucose exit flux by varying concentrations of maltose (*see* Fig. 3) in the external solution at 0.1 MPa and at 40 mPa was simulated as in Fig. 10. The parameters used (Table 3) are similar to those in Fig. 10 and Table 2. Additional parameters are K_{wm} and $K_{maltose}$, the dissociation constants of water for the maltose binding site and of maltose. The simulated K_i for [maltose] inhibition of glucose exit at the external site at 0.1 MPa is 0.35 mM, (two-site) and 0.38 mM (carrier); V_{max} = 0.084 sec^{-1} and 0.074 (carrier); at 40 MPa, K_i = 0.11 mM (carrier) and 0. 10 mM (two-site), V_{max} = 0.059 sec^{-1} (2-site) and 0.056 sec^{-1}(carrier). The simulated activation volumes show biphasic responses to [maltose] with optimal increases at around 250 μM maltose; thereafter, the activation volumes decrease with [maltose].

Glucose transport can be modelled in two ways. Firstly as a two-sites model, where net glucose flow is assumed to occur as a result of the ligand hopping from a filled site on the *cis* side to a vacant site on the *trans* side. The mobility of ligand movement between sites can be altered by conformational changes involving hydration. The second way of modelling glucose transport is based on the conventional carrier model. Occupied *cis*-facing sites alternate with equivalent *trans*-facing sites. As the whole assembly of ligand and binding sites alternates between sides, there is no relative motion between transporter and ligand during translocation across the membrane. Addition of the hydrated substates, *CW* and *CGW* introduces more degrees of freedom into both fixed site and alternating carrier

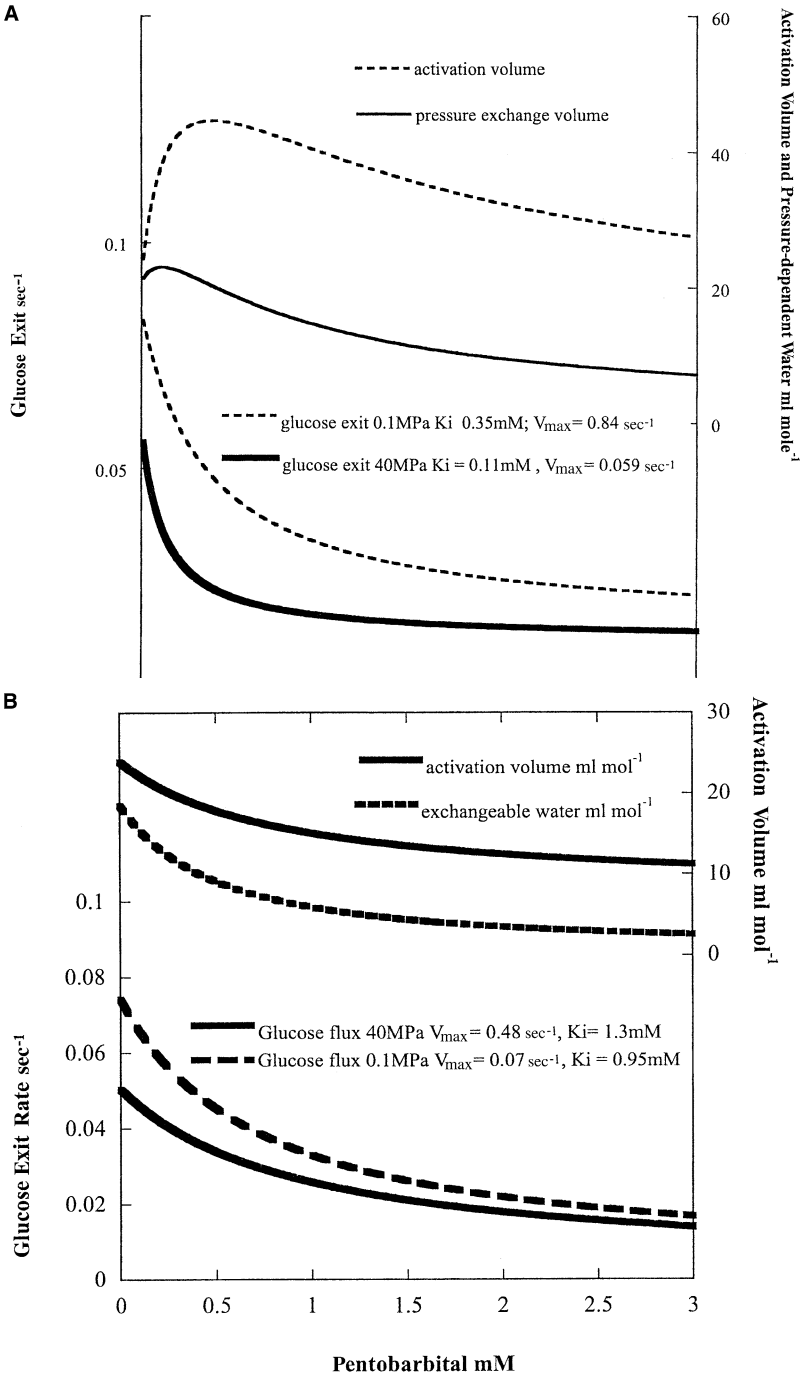

Fig. 12. Simulation of effects of pressure and pentobarbital on glucose exit kinetics and activation volume. (*A*) Simulation of effects of pressure on pentobarbital exit using/two-site model. (*B*) Simulation of effects of pressure on pentobarbital-dependent inhibition of glucose exit and activation volume. Inhibition of glucose exit flux by varying concentrations of pentobarbital in the external solution at 0.1 MPa and at 40 MPa was simulated as in Fig. 4. Table 4 gives the parameters used. Additional parameters are $K_{wpentobarb}$ and $K_{pentobarb}$, the dissociation constants of water for the pentobarbital binding site and of pentobarbital. The simulated K_i for [pentobarbital] inhibition of glucose exit at the external site at 0.1 MPa is 1.0 mM, V_{max} = 0.069) and at 40 MPa, K_i = 2.0 mM, V_m = 0.047 sec^{-1} (thin continuous line). The simulated pressure-displaceable and activation volume decreases from 20 ml mol^{-1} at 0 mM pentobarbital to 5–8 ml mol^{-1} at 2.5 mM pentobarbital. These data are similar to those obtained in Fig. 4.

models of glucose transport. Both models provide equally satisfactory descriptions of the kinetics of glucose flows in all the conditions described in this paper and also for observed activation volume changes. Previous experiments comparing net and exchange rates of 3-O-methyl glucose and mannose in rat erythrocytes favour the two-site model, (Naftalin & Rist, 1994; Naftalin, 1996). However, these conclusions do not consider hydrated intermediate forms of the carrier.

The Hydration Model also Explains Accelerated Exchange Flux of Glucose

The conventional explanation for the higher V_{max} and K_m of *accelerated equilibrium exchange* than for *net flux*, is that glucose-liganded transporter crosses with higher mobility in parallel with the slower transit of the empty carrier (Lieb and Stein, 1970; LeFevre, 1973; Stein, 1986; Baker & Widdas, 1988; Naftalin & Rist, 1994). Consequently, *cis-trans* net flux leads to

empty carrier depletion on the *cis* side and its accumulation on the *trans* side. Sugar added to the *trans* side reduces the asymmetric carrier distribution by returning carrier to the *cis* side and hence increases unidirectional exit flux.

The explanation of *accelerated exchange* flux with fixed binding sites is that bilateral sugar binding causes a conformational change in the transporter, which increases ligand mobility within the transporter, hence the exchange transport process is more rapid than net transport (Naftalin & Rist, 1994). A modification of this view is that there is cooperative interaction between GLUT1 dimers. The coupled pairs of asymmetric alternating carriers behave in a similar way to a two-site model (Sultzman & Carruthers, 1999).

The current models of glucose transport incorporating hydration also account for *accelerated exchange transport* and related phenomena such as *countertransport* (Rosenberg & Wilbrandt, 1957). Ligand and solvent exchanges between solutions and transporter binding sites are 3–4 orders of magnitude faster ($\tau \approx 100$ nsec^{-1}) than *accelerated exchange rates* across any transporter (Huber, Klingenberg & Beyer, 1999; Janoshazi & Solomon, 1993) ($\tau \approx 1$ msec^{-1}). Consequently, equilibria between the solvent and ligands in solutions and the adjacent binding sites on the transporter surface are unaffected by sugar transits across the transporter. The rates of large-scale protein unfolding are of the order, $\tau \approx 100$ μsec^{-1} (Deniz et al., 2000). The lifetime of the hydrated unfolded state permits approximately 1000 ligand exchanges between the sites and solution during each unfolding event. Hence rapid glucose isotope exchange between the bound state and the adjacent solution occurs without displacement of water (Fig. 5).

Retention of the hydrated state between successive ligand exchanges ensures that the unidirectional flux of sugar in the accelerated exchange mode is mainly in the bilateral hydrated state. During *zero trans* net flux the transporter becomes partially dehydrated, as is evident from the lower activation volume change (≈30 ml mol^{-1}) during *zero trans net exit* than during *exchange flux* (74 ± 2 ml mol^{-1}) (Thorne et al., 1992) or *infinite cis efflux*, ≈60 ml mol^{-1} (Fig. 2) and therefore has a lower mobility (Fig. 5). A lower activation energy for *accelerated exchange* than for net glucose flux has often been observed and is consistent with exchange taking place between the hydrated states with higher glucose mobility than during *zero trans* net flux (Appleman and Leinhard, 1989; Naftalin & Rist, 1994; Naftalin & Arain, 1999). Increasing the dissociation constants K_w and K_{gw} of water binding to carrier and to the glucose-transporter complex from 10 M at 0.1 MPa to 25 M at 40 MPa simulates the effects of raising pressure with both carrier and fixed-site models. Both the hydrated carrier and the fixed-site models give excellent simulations of all the phenomena observed here (*see* Table 1; Figs. 2, 10*A* and 10*B*, 11*A* and 11*B*, 12*A* and 12*B*).

Table 1. Summary of effects of pressure on parameters of sugar transport across GLUT1 transporter at 25°C

Condition	K_i	V_m	Activation volume	Reaction volume
Net glucose exit (*infinite cis exit*)	▼	▼	▲	▼
Maltose inhibition of glucose exit	▼	▼	▲▼	▼
Pentobarbital inhibition of glucose exit	▲	▼	▼	▲
Sorbose exit	No effect	No effect	No effect	—

Effects of Maltose on Glucose Exit and Activation Volume

The pressure-dependent increase in maltose affinity (Fig. 3) indicates that hydration (reduced by raised pressure) of the external site reduces maltose affinity. The biphasic increase in hydration at low external [maltose] followed by reversal of the hydration response to binding of intracellular glucose at higher maltose concentrations suggests that when maltose binds to unhydrated sites it exposes them to hydration. However, once maltose binds to these hydrated sites it appears to occlude them and prevents pressure displacement of water. The carrier-model simulation of raised pressure from 0.1 MPa to 40 MPa is achieved by raising K_w from 5 to 25 M, raising K_{wg} from 10 M to 15 M, but K_{wm} is unaltered at 10 M. In the two-site-model simulations raised pressure is simulated by changing K_w from 10 M–50 M and K_{wg} from 12 to 25 M, but again K_{wm} remains at 45 M at both pressures, (Fig. 11*A* and 11*B*). Widdas and Baker (1992) reported similar protective effects with maltose on methanol-dependent inhibition of glucose exit. These findings show consistency with the effects of raised external glucose (Fig. 10*A* and 10*B*), in that response to pressure of K_w and K_{wg} is similar in both kinds of simulation. A key point of interest with these experiments is the biphasic hydration response with maltose. This strongly resembles the biphasic response of 3-O-methyl-glucose entry into red cells with raised maltose and the biphasic rates of cytochalasin B binding to the inside sites with raised maltose (Hamill et al., 1999; Sultzman & Carruthers, 1999). The unexpected biphasic effect of maltose on sugar transport across GLUT1 and the biphasic effects of maltose on the rate of cytochalasin B binding to the inside can now be explained. Maltose binding at low concentrations to its high-affinity unhydrated site promotes hydration and consequently increases mobility of the transported sugars. At higher concen-

Table 2. Parameters used for the simulations in Fig. 10

Two-Site-model parameters	0.1 MPa	40 MPa	Carrier-model parameters	0.1 MPa	40 MPa
k_1	0.015 sec^{-1}	0.015 sec^{-1}	R_w	0.1 sec^{-1}	0.1 sec^{-1}
k_2	0.1 sec^{-1}	0.1 sec^{-1}	R_g	5 sec^{-1}	5 sec^{-1}
k_3	0.15 sec^{-1}	0.15 sec^{-1}	R_{gw}	10 sec^{-1}	10 sec^{-1}
K_{water}	10 M	25 M	K_{water}	5 M	25 M
$K_{glucose}$	1.2 mM	1.2 mM	$K_{glucose}$	1 mM	1
K_{wg}	10 M	25 M	K_{wg}	10 M	15 M

Table 3. Parameters used for the simulations in Fig. 11

Two-Site-model parameters	0.1 MPa	40 MPa	Carrier-model parameters	0.1 MPa	40 MPa
k_1	0.01 sec^{-1}	0.01 sec^{-1}	R_w	0.1 sec^{-1}	0.1 sec^{-1}
k_2	0.12 sec^{-1}	0.12 sec^{-1}	$R_{glucose}$	5 sec^{-1}	5 sec^{-1}
k_3	0.15 sec^{-1}	0.15 sec^{-1}	R_{gw}	10 sec^{-1}	10 sec^{-1}
K_{water}	12 M	25 M	K_{water}	5 M	25 M
$K_{glucose}$	0.6 mM	0.6 mM	$K_{glucose}$	1.2 mM	1.2 mM
K_{wg}	10 M	50 M	K_{wg}	10 M	15 M
K_{wm}	40 M	40 M	K_{wm}	10 M	10 M
$K_{maltose}$	0.06 mM	0.06 mM	$K_{maltose}$	0.03 mM	0.03 mM

Table 4. Parameters used for the simulations in Fig. 12

Two-Site parameters	0.1 MPa	40 MPa	Hydrated carrier parameters	0.1 MPa	40 MPa
k_1	0.012 sec^{-1}	0.012 sec^{-1}	R_w	0.1 sec^{-1}	0.1 sec^{-1}
k_2	0.1 sec^{-1}	0.1 sec^{-1}	$R_{glucose}$	5 sec^{-1}	5 sec^{-1}
k_3	0.15 sec^{-1}	0.15 sec^{-1}	R_{gw}	10 sec^{-1}	10 sec^{-1}
K_{water}	10 M	25 M	K_{water}	5 M	40 M
$K_{glucose}$	1.2 mM	1.2 mM	$K_{glucose}$	1.2 mM	1.2 mM
K_{wg}	15 M	25 M	K_{wg}	10 M	25 M
$K_{wpentobarb}$	25 M	25 M	$K_{wpentobarb}$	10 M	10 M
$K_{pentobarb}$	0.1 mM	0.3 mM	$K_{pentobarb}$	0.1 mM	0.4 mM

trations, when maltose binds to hydrated sites, it occludes the water in the site, thereby inhibiting transport and preventing pressure displacement of water from the site.

Effects of Pentobarbital on Activation Volume

The effects of pentobarbital are consistent with it preventing the glucose-dependent increases in hydration of the transporter (Figs. 4, 12*A* and 12*B*). This is consistent with the previous findings that pentobarbital is a mixed inhibitor of glucose transport and its inhibition of the glucose-dependent decrease in activation energy of glucose exit (Naftalin & Arain, 1999). The effects of raised pressure alone on glucose exit are similar to those induced by pentobarbital alone in that both cause a mixed inhibition of glucose exit. However, whereas raised pressure increases the affinity of glucose (Fig. 2), pentobarbital reduces it (Naftalin & Arain, 1999). It can be predicted that pentobarbital-like raised pressure prevents glucose-dependent increases in hydration of the transporter and hence pentobarbital eliminates the effects of pressure. The effects of pentobarbital on glucose exit are simulated (Fig. 12*A*, *B*) by assuming that pentobarbital binds with high affinity to unhydrated sites and that its affinity is reduced when the sites are hydrated. Raised pressure also raises the K_i of pentobarbital inhibition of glucose exit from 1 mM to 2.57 mM (Fig. 4). Using the carrier model, simulation of the data on changing pressure from 0.1 MPa to 40 MPa is obtained by raising the K_d of pentobarbital for the unhydrated pentobarbital-binding site from 0.11 mM to 0.4 mM. Similar effects are obtained with the 2-fixed-site model. Again, simulation on raising pressure from 0.1 MPa to 40 MPa is ob-

tained by a decrease in water affinity K_w from 10 to 25 M and K_{wg} from 15 to 25 M. However, K_{wp} = 25 M remains unaltered with pressure.

Conclusions

A model is presented, in which glucose transport is mediated by a transporter capable of binding glucose in a high-affinity unhydrated form or in a low-affinity hydrated form on both sides of the membrane. Transport rates between the hydrated low-affinity forms of the transporter are faster than between unhydrated forms.

The model accounts for the higher activation volumes and lower activation energies of glucose-bound states such as *infinite cis* net exit or *accelerated exchange* flux. It also accounts for both the observed increases in affinity of glucose and maltose and decrease in V_{max} of *zero trans* net glucose exit with raised pressure. It also may account for the mixed inhibitory effects of barbiturates. These models make some straightforward and testable hypotheses about the nature of hydration interactions with the transporter. Ultimately it may be possible to discriminate between the two-fixed-site or the alternating-fixed-site models using methods that monitor water-and solute-binding directly.

The authors are grateful to the Wellcome Trust for financial support and to the Arthritis Research Campaign (W0604) (RJW).

References

Appleman, J.R., Lienhard, G.E. 1989. Kinetics of the purified glucose transporter. Direct measurement of the rates of interconversion of transporter conformers. *Biochemistry* **28:**8221–8227

Baker, G.F., Widdas, W.F. 1988. Parameters for 3-O-methyl glucose transport in human erythrocytes and fit of asymmetric carrier kinetics. *J. Physiol.* **395:**57–76

Baker, G.F., Widdas, W.F. 1991. High concentrations of methanol eliminate the modifier site activity of the red cell glucose transporter. *J. Physiol.* **438:**272P

Browning, J.A., Walker, R.E., Hall, A.C., Wilkins, R.J. 1999. Modulation of Na^+ x H^+ exchange by hydrostatic pressure in isolated bovine articular chondrocytes. *Acta. Physiol. Scand.* **166:**39–45

Carruthers, A. 1990. Facilitated diffusion of glucose. *Physiol. Rev.* **70:**1135–1176

Cioni, P., Strambini, G.B. 1999. Pressure temperature effects on protein flexibility from acrylamide quenching of protein phosphorescence. *J. Mol. Biol.* **291:**955–964

Deniz, A.A., Laurence, T.A., Beligere, G.S., Dahan, M., Martin, A.B., Chemla, D.S., Dawson, P.E., Schultz, P.G., Weiss. S. 2000. Single-molecule protein folding diffusion fluorescence resonance energy transfer studies of the denaturation of chymotrypsin inhibitor 2. *Proc. Natl. Acad. Sci.* **97:**5179–5184

Ebel. C., Eisenberg, H. Ghirlando, R. 2000 Probing protein-sugar interactions. *Biophy. J.* **78:**385–393

El-Barbary, A., Fenstermacher, J.D., Haspel, H.C. 1996. Barbiturate inhibition of GLUT-1 mediated hexose transport in human erythrocytes exhibits substrated dependence for equilibrium exchange but not unidirectional sugar flux. *Biochemistry.* **35:**15222–15227

Fersht, A. 1999. *In:* Structure and Mechanism in Protein Science. Ch. 2, p 73 W.H. Freeman and Co. New York

Fischbarg, J., Min, C., Li, J., Iserovich, P., Czegledy, F., Kuang, K.Y., Garner, M. 1994. Evidence that the glucose transporter serves as a water channel in J774 macrophages. *Mol. Cell. Biochem.* **140:**147–l62

Gross, M., Auerbach, G., Jaenicke, R. 1993. The activities of monomeric enzymes show complex pressure-dependence. *FEBS Lett* **321:**256–260

Gross, M., Jaenicke, R. 1994 Proteins under pressure. The influence of high hydrostatic pressure on structure, function and assembly of proteins and protein complexes. *Eur. J. of Biochem.* **221:**617–620

Hamill, S., Cloherty, E.K., Carruthers, A. 1999. The human erythrocyte sugar transporter presents two sugar import sites. *Biochemistry.* **38:**16974–16983

Hartnig, C., Witschel, W., Spohr, E., Gallo, P., Ricci, M.A., Rovere, M., 2000. Modiflcations of the hydrogen bond network of liquid water in a cylindrical SiO_2 pore. *J. Mol. Liquids* **85:**127–137

Huber, T., Klingenberg, M., Beyer, K. 1999. Binding of nucleotides by the mitochondrial ADP/ATP carrier as studied by 1H nuclear magnetic resonance spcctroscopy. *Biochemistry.* **38:**762–769

Janoshazi, A., Solomon, A.K. 1993. Initial steps of alpha- and beta-D-glucose binding to intact red cell membrane. *J. Membrane. Biol.* **132:**167–178

LeFevre, P.G. 1973. A model for erythrocyte sugar transport based on substrate-conditioned "introversion" of binding sites. *J. Membrane. Biol.* **11:**1–9

Lieb, W.R., Stein, W.D. 1970. Quantitative predictions of a non-carrier model for glucose transport across the human red cell membrane. *Biophys. J.* **10:**585–609

Mannuzzu, L.M., Moronne, M.M., Macey, R.I. 1993. Estimate of the number of urea transport sites in erythrocyte ghosts using a hydrophobic mercurial. *J. Membrane. Biol.* **133:**85–97

Mitchell, D.C., Litman, B.J. 1999. Effect of protein hydration on receptor conformation; decreased levels of bound water promote metarhodopsin II formation. *Biochemistry.* **38:**7617–7623

Mitchell, D.C., Litman, B.J. 2000. Effect of ethanol and osmotic stress on receptor conformation. Reduced water activity amplifies the effect of ethanol on metarhodopsin II formation. *J. Biol. Chem.* **275:**5355–5360

Naftalin, R.J., Holman, G.D. 1977 *In*: Membrane Transport in Red Cells. J.C. Ellory, V.L. Lew, editors. pp. 257–300. Academic Press. New York.

Naftalin, R.J., Rist, R.J. 1991. 3-O-methyI-D-glucosc transport in rat red cells: effects of heavy water. *Biochim. Biophys. Acta* **1064:**37–48

Naftalin, R.J., Rist, R.J. 1994. Reexamination of hexose exchanges using rat erythrocytes — evidence inconsistent with a one-site sequential exchange model, but consistent with a 2-site simultaneous exchange model. *Biochim. Biophys. Acta* **1191:**65–78

Naftalin, R.J. 1996. Evidence from studies of temperature-dependent changes of D-glucose, D-mannose and L-sorbose permeability that different states of activation of the human erythrocyte hexose transporter exist for good and bad substrates. *Biochim. Biophys. Acta* **1328:**13–29

Naftalin, R.J., Arain, M. 1999. Interactions of sodium pentobarbital with D-glucose and L-sorbose transport in human red cells. *Biochim. Biophys. Acta* **1419:**78–88

Northrop, D.B. 1996. *In:* High Pressure Effects in Molecular Biology and Enzymology. J.A. Markely, C.A. Royer, D.B. Northrop, Editors, pp. 221-224. Oxford University Press, New York

Northrop, D.B., Cho, Y.K. 2000. Effect of pressure on deuterium isotope effects of yeast alcohol dehydrogenase: evidence for mechanical models of catalysis. *Biochemistry*. **39:**2406–2412

Parsegian, V.A., Rand, R.P., Rau, D.C. 2000. Osmotic stress, crowding, preferential hydration, and binding: A comparison of perspectives. *Proc. Natl. Acad. Sci. USA* **97:**3987–3992

Rand, R.P., Fuller, N.L., Butko, P., Francis, G., Nicholls, P. 1993. Measured change in protein solvation with substrate binding and turnover. *Biochemistry* **32:**5925–5929

Reid, C., Rand, R.P. 1997. Probing protein hydration and conformational states in solution. *Biophys. J.* **72:**1022–1030

Rosenberg, T., Wilbrandt, W. 1957. Uphill transport induced by counterflow. *J. Gen. Physiol.* **41:**289–96

Sen, A.K., Widdas, W.F. 1962. Determination of the temperature and pH dependence of glucose transfer across the human erythrocyte membrane measured by glucose exit. *J. Physiol.* **160***:*392–403

Stein, W.D. 1986 *In:* Transport and Diffusion across Cell Membranes. Chapter 4 pp. 231–262 Academic Press, London

Stephenson, K.N., Croxen, R.L., El-Barbary, A., Fenstermacher, J.D., Haspel, H.C. 2000. Inhibition of glucose transport and direct interactions with type 1 facilitative glucose transporter (GLUT-1) by etomidate, ketamine, and propofol: a comparison with barbiturates. *Biochem. Pharmacol.* **60:**651–659

Sultzman, L.A. and Carruthers, A. 1999. Stop-flow analysis of cooperative interactions between GLUT1 sugar import and export sites. *Biochemistry*. **38:**6640–6650

Svergun, D.I. Richard, S., Koch, M.H.J., Sayers, Z., Kuprin, S., Zaccai, G. 1998. Protein hydration in solution: Experimental observation by x-ray and neutron scattering. *Proc. Natl. Acad. Sci. USA*. **95:**2267–2272

Thorne, S.D., Hall, A.C., Lowe, A.G. 1992. Effects of pressure on glucose transport in human erythrocytes. *FEBS. Lett*. **301:**299–302

Timasheff, S.N. 1998. Control of protein stability and reactions by weakly interacting cosolvents: the simplicity of the complicated. *Adv. Protein. Chem*. **51:**355–432

Villa, J., Strajbl, M., Glennon, T.M., Sham, Y.Y., Chu, T.Z., Warshel, A. 2000. How important are entropic contributions to enzyme catalysis? *Proc. Natl. Acad. Sci.* **97:**11899–11904

White, S.H., Wimley, W.C. 1999. Membrane protein folding and stability: physical principles. *Annu. Revs. Biophys. Mol. Structure* **28:**319–365

Widdas, W.F., Baker, G.F. 1992. The action of maltose on glucose exits in human erythrocytes in the presence of high concentrations of methanol. *J. Physiol.* **446:**174P

Widdas, W.F., Baker, G.F. 1998. The physiological properties of human red cells as derived from kinetic osmotic volume changes. *Cytobios.* **95:**173–201

Xie, G., Timasheff, S.N. 1997. The thermodynamic mechanism of protein stabilization by trehalose. *Biophys. Chem.* **64:**25–43

Zeidel, M.L., Albalak, A., Grossman, E., Carruthers, A. 1992. Role of glucose carrier in human erythrocyte water permeability. *Biochemistry* **31:**589–596

Zeng, H., Parthasarathy, R., Rampal, A.L., Jung, C.Y. 1996. Proposed structure of putative glucose channel in GLUT1 facilitate glucose transporter. *Biophys. J.* **70:**14–21